

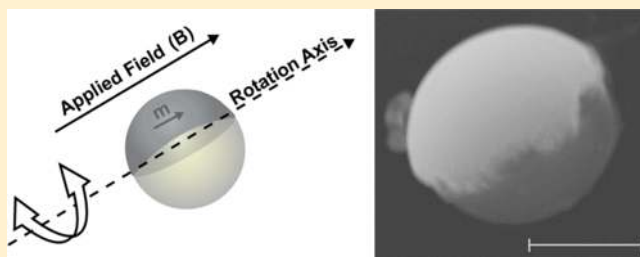
Experimental System for One-Dimensional Rotational Brownian Motion

Brandon H. McNaughton,^{*,†,‡} Paivo Kinnunen,^{‡,§} Miri Shlomi,[‡] Codrin Cionca,[§] Shao Ning Pei,[‡] Roy Clarke,[§] Panos Argyrakis,[‡] and Raoul Kopelman^{*,†,‡,§}

[†]Department of Biomedical Engineering, [‡]Department of Chemistry, and [§]Department of Physics University of Michigan, Ann Arbor, Michigan 48109, United States

S Supporting Information

ABSTRACT: We present here an experimental, strictly one-dimensional rotational system, made by using single magnetic Janus particles in a static magnetic field. These particles were half-coated with a thin metallic film, and by turning on a properly oriented external static magnetic field, we monitor the rotational Brownian motion of single particles, in solution, around the desired axis. Bright-field microscopy imaging provides information on the particle orientation as a function of time. Rotational diffusion coefficients are derived for one-dimensional rotational diffusion, both for a single rotating particle and for a cluster of four such particles. Over the studied time domain, up to 10 s, the variation of the angle of rotation is strictly Brownian; its probability distribution function is Gaussian, and the mean squared angular displacement is linear in time, as expected for free diffusion. Values for the rotational diffusion coefficients were also determined. Monte Carlo and hydrodynamic simulations agree well with the experimental results.



INTRODUCTION

Diffusion has been one of the most fundamental and well studied processes in physical science, with a long history, starting with the observation made by Brown in 1827,^{1,2} of pollen particles floating on water. It was later described using thermodynamics by Einstein in 1906,^{3–5} and implemented by Perrin to determine Avogadro's number in 1910.⁶ These fundamental developments used basic Brownian translation and rotation as models for the study of diffusion mechanisms^{7–9} which over the years have led to a plethora of applications in practically all scientific fields, including physics, nanoscience, chemistry, biology, and economics. One can appreciate the significance of studying Brownian kinetics and other stochastic problems by the fact that the numerical values of the relevant spatial parameters scale from the stars¹⁰ to the nanoscale.¹¹ While the translational Brownian motion is better known and more often used, Brownian rotation has also been extensively studied.¹²

The fundamental distinction between the commutative one-dimensional and the noncommutative three-dimensional rotational motion was not addressed until Furry's work in 1957.¹³ Thus, the standard formula, for the mean-squared displacement, $\langle R^2 \rangle \sim t$, is valid, only in the short-time limit, while rigorously applicable, at all times, only to one-dimensional Brownian rotation. Therefore, having such a strictly one-dimensional Brownian rotation system is of both theoretical and practical significance.

In the past, progress has been made toward a free one-dimensional Brownian rotation system;^{14,15} however, there has

been a lack of direct measurements, especially for a single particle, when it comes to truly one-dimensional Brownian rotation systems, i.e., systems that are rotating freely only about a fixed axis. For example, Kappler¹⁶ suspended a mirror with carbon wires and monitored light reflections from the mirror. Cheng and colleagues^{17,18} trapped disk-like colloids in optical tweezers. In these experiments, the objects that undergo one-dimensional rotation are kept from freely rotating, e.g., they are in a potential that opposes their one-dimensional rotation. In the case of Kappler, the mirror cannot turn freely. In the case of Cheng et al., a potential resisting rotation is created by the optical trap. More recently, Altintas and colleagues were able to implement magnetic clamping to confine the diffusion of individual nanorods.¹⁵ Additionally, systems have been utilized to study the coupling between translational and rotational diffusion.^{19,20} However, all of the above systems require a significant restriction on the translational motion and/or the rotational motion about the confined axis, such that a “passive” restoring force inhibits free diffusion. Furthermore, the systems sometimes require more than one particle and the experiment cannot be performed on a single particle. Therefore, in this study, we demonstrate and

Special Issue: Shaul Mukamel Festschrift

Received: August 2, 2010

Revised: November 29, 2010

Published: April 18, 2011

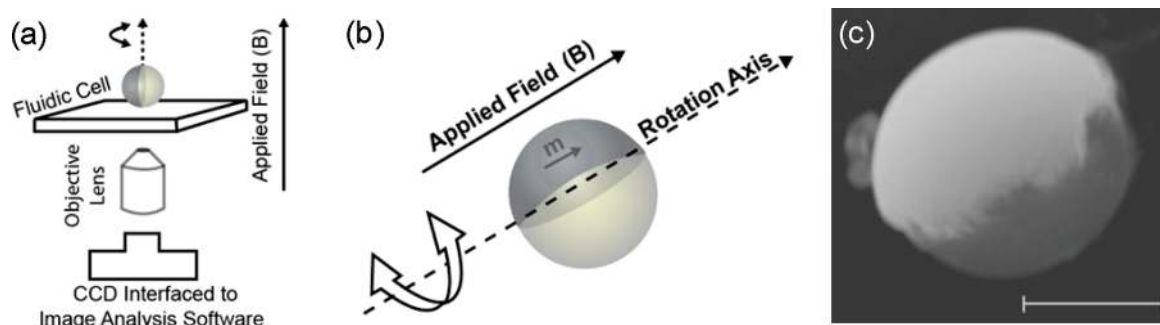


Figure 1. Schematic representation of (a) the experimental setup used to observe the one-dimensional rotation of a single Janus particle and (b) the concept underlying the one-dimensional rotation of a magnetic microsphere. (c) Scanning electron microscopy image of a single magnetic Janus particle, where the scale bar is $1 \mu\text{m}$.

experimentally validate one-dimensional rotational diffusion for a single particle, as well as for an aggregate.

To create and actively control a one-dimensional rotator that is free to diffuse through all angles in a plane (about one fixed axis), we have designed a system that implements magnetic Janus particles,^{21–23} see Figure 1. Janus particles have two chemically or physically different hemispheres.²³ Here, we orient such a magnetic particle in a static magnetic field so that rotational diffusion can be observed with standard bright-field microscopy.

One approach to fabricating magnetic Janus particles is to deposit a thin metallic layer onto half of a nonmagnetic particle. We have been using this type of Janus particle in our laboratory, where the optical asymmetry of the particle has previously been used to measure the particle orientation as a function of time.^{22,24–28} Due to the magnetic content, the particle can be magnetized in a variety of directions and can be manipulated both translationally and rotationally. Magnetic and nonmagnetic Janus particles have been used for a variety of applications, such as single bacterial cell detection²⁸ and for the study of Brownian rotational dynamics.^{29–32} Recently, Hong and colleagues were able to use an assembly of four such particles to study the rotational diffusion about two axes of a rod-shaped particle.³¹ They measured the diffusion coefficient along each axis of the rod when its rotation was restricted at a glass-fluid interface. This approach works well for particles with a strict rod-like symmetry, but there remains a need for a method that can actively isolate the two axes of rotation for particles that are symmetric and for arbitrary particle shapes that exhibit diffusion when at an interface (i.e., any aggregate that does not have rod-like symmetry). Furthermore, actively restricting the rotational diffusion is required when the aggregate is in suspension and can diffuse to the bulk solution at a significant distance from an interface. Therefore, we have designed a system that enables the measurement of one-dimensional Brownian rotational dynamics, i.e., rotation around a single fixed axis.

EXPERIMENTAL METHODS

One-dimensional rotation refers to the isolation of the rotational motion to being around a single axis. This was accomplished by utilizing a static magnetic field to restrict the motion of single Janus particles to rotation around this single, fixed axis. To monitor the orientation, the magnetic microsphere was fabricated by coating a nonmagnetic microsphere with a thin metallic layer, see Figure 1. This metallic layer provides an optical

asymmetry and, depending on the rotational axis, creates a modulated intensity (with magnetic field applied parallel to imaging plane) or a constant intensity with changing angular orientation (magnetic field applied perpendicular to imaging plane). A unique feature of this method is that the rotational axis of choice can be actively isolated and arbitrarily chosen. This depends on the initial magnetization of the particle and the strength and orientation of the applied field (here a diffusion plane parallel to the sample plane was chosen). The static magnetic field was established with two Helmholtz coils (a total of four electromagnets) to control the orientation of the particle. Typical magnetic fields were 10 Oe and applied through only one set of Helmholtz coils.

Spherical polystyrene particles with a $0.5\text{--}2 \mu\text{m}$ diameter were dispersed onto a glass substrate and coated by evaporating, from one side, a nickel layer of 200 nm thickness (this process is described in detail in ref 33). The result is a two hemisphere particle, where one surface is polystyrene and the other is nickel. The nickel could also potentially be used to study catalytic properties and anomalous diffusion.³⁴ In cases of biological applications, an additional layer of gold can be coated onto the particle. The magnetic particles were suspended in doubly deionized water with a $<0.5\%$ concentration of surfactant sodium dodecyl sulfate (to minimize stiction). A $100\times$ oil immersion objective lens on an inverted Olympus (IX71) microscope was used, in bright-field mode, to image the particles. Images were obtained using a Coolsnap CCD camera. Image analysis was performed using ImageJ software.³⁵ Each particle's bright and dark spots, arising from the effect of light passing through, or being blocked by, the two different types of hemispheres, were tracked using an ImageJ routine, MultiTracker (see images in Figure 4). From the tracking values, the orientation of the particle was measured in time. Software from OriginLab was then used to analyze the angular displacement and to perform fitting. To minimize surface interactions, and any effects from having a displaced center of mass, we applied a magnetic field along the optical axis (instead of in the imaging plane). In a separate series of tests the extent of the magnetic confinement was quantified by applying a magnetic field parallel to the image plane and using a magnetic particle with a 100 nm nickel layer. The particle was magnetized through the poles in order to measure the magnetic confinement; when a field was applied in the imaging plane, the particle aligned with the hemispheres in-line with the field and in this way the confinement can be quantified; see Figure 2.

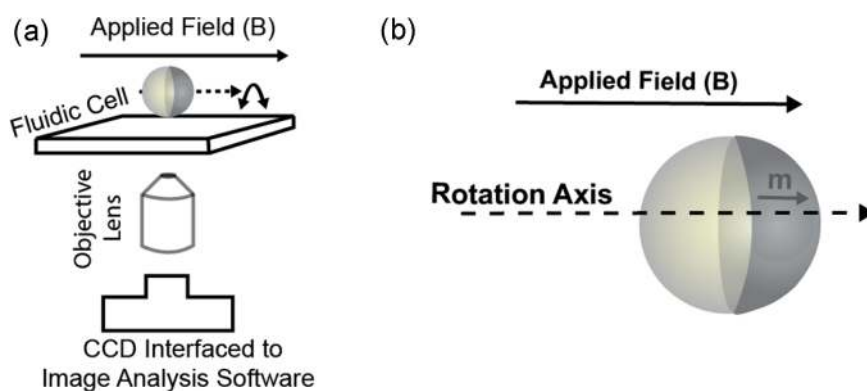


Figure 2. Schematic representation of (a) the experimental setup used to observe one-dimensional confinement of a single Janus particle and (b) the concept underlying one-dimensional confinement of a magnetic microsphere.

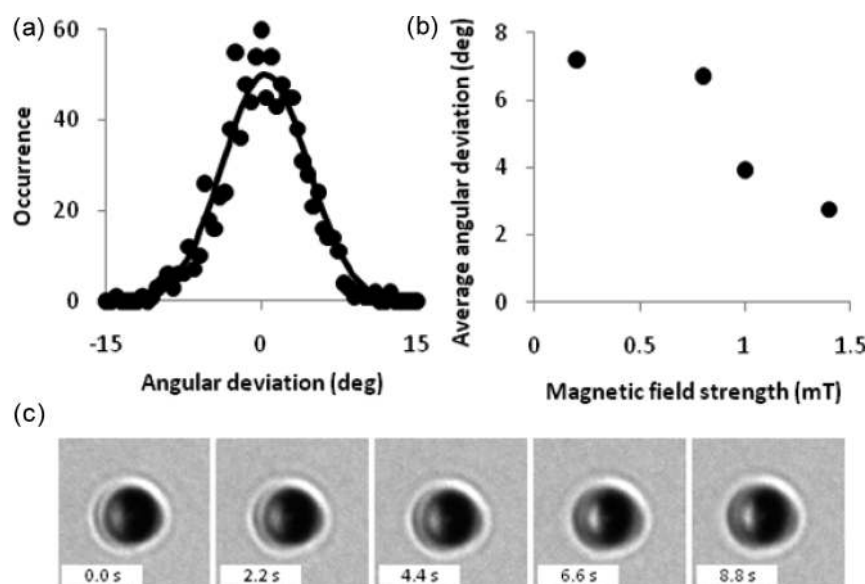


Figure 3. Quantification of the angular confinement. Experimental results for a single particle that was magnetized through the poles and in a static magnetic field applied in the sample plane for the (a) relative angular position in the presence of a 1.0 mT field, resulting in an angular deviation of 3.9° and (b) the effect of increased magnetic field amplitude on the extent of confinement. (c) Time series of microscopy images (taken at 100 fps), where the image is $7 \mu\text{m} \times 7 \mu\text{m}$.

RESULTS AND DISCUSSIONS

In one-dimensional systems, the time dependence of the rotational mean squared displacement equation, is given by

$$\langle \theta^2 \rangle = 2D_r t \quad (1)$$

where D_r is the rotational diffusion coefficient:

$$D_r = \frac{kT}{\gamma} = \frac{kT}{\kappa\eta V} \quad (2)$$

Here, k is the Boltzmann constant, T is temperature, γ is the rotational drag, κ is the shape factor, η is the dynamic viscosity, and V is the particle volume. For three-dimensional rotational systems, it has been shown that more intricate equations are needed,^{13,36,37} due to the noncommutation of rotations in three-dimensional space. Often, rotation is measured on a system with high enough symmetry to allow a quasi-one-dimensional analysis.^{29–31,38,39} Also, with more complex shapes and aggregates, the diffusion coefficient cannot be found analytically.⁴⁰

Angular displacements resulting from commutative Brownian steps will generally have a Gaussian distribution. Here we utilize the one-dimensional rotational probability function⁴¹

$$P(d) = \frac{1}{2\pi\sigma^2} \exp\left(-\frac{d^2}{2\sigma^2}\right) \quad (3)$$

where d is the angular displacement and σ is the root-mean-square deviation. σ is governed by the diffusivity (coefficient of angular diffusion)

$$\sigma = \sqrt{2Dt} \quad (4)$$

where t is the time interval between angular displacements.

In order to measure the extent of the magnetic particle confinement, we used particles with a magnetization along the equator (as compared to the particles in Figure 1 magnetized through the poles) and applied a magnetic field in the sample plane (see the Experimental Section and Figure 2 for details). Due to the arrangement of the magnetic moment and applied

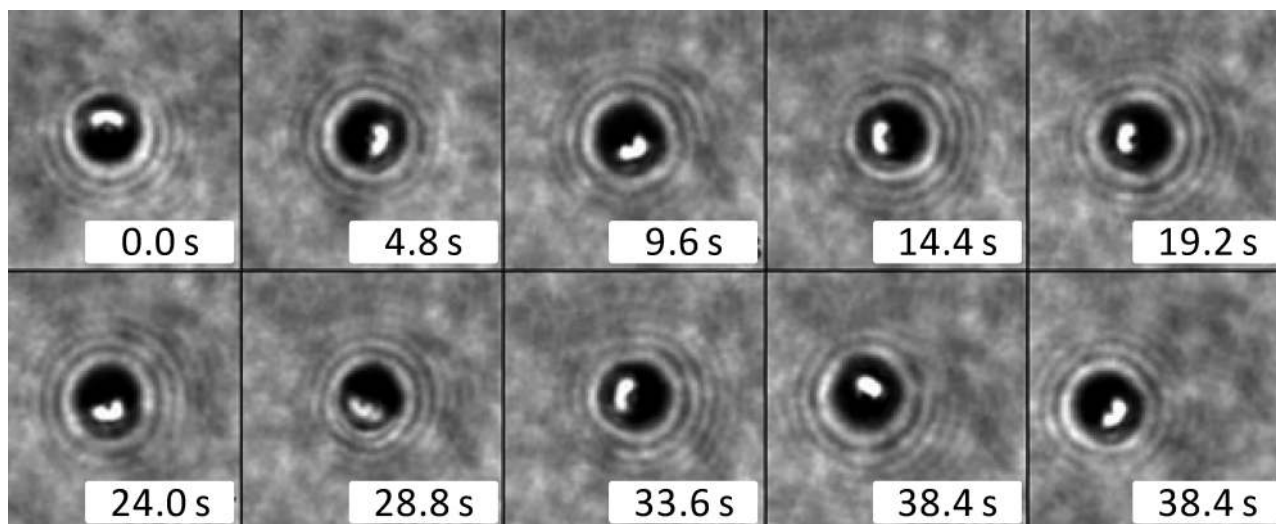


Figure 4. Bright field microscopy images of one-dimensional Brownian rotation of a single $2.0\ \mu\text{m}$ diameter microsphere rotating around a fixed axis that is parallel to the optical axis (perpendicular to the imaging plane). The images are shown for every 220th frame (4.8 s intervals), where the image size is approximately $7\ \mu\text{m} \times 7\ \mu\text{m}$.

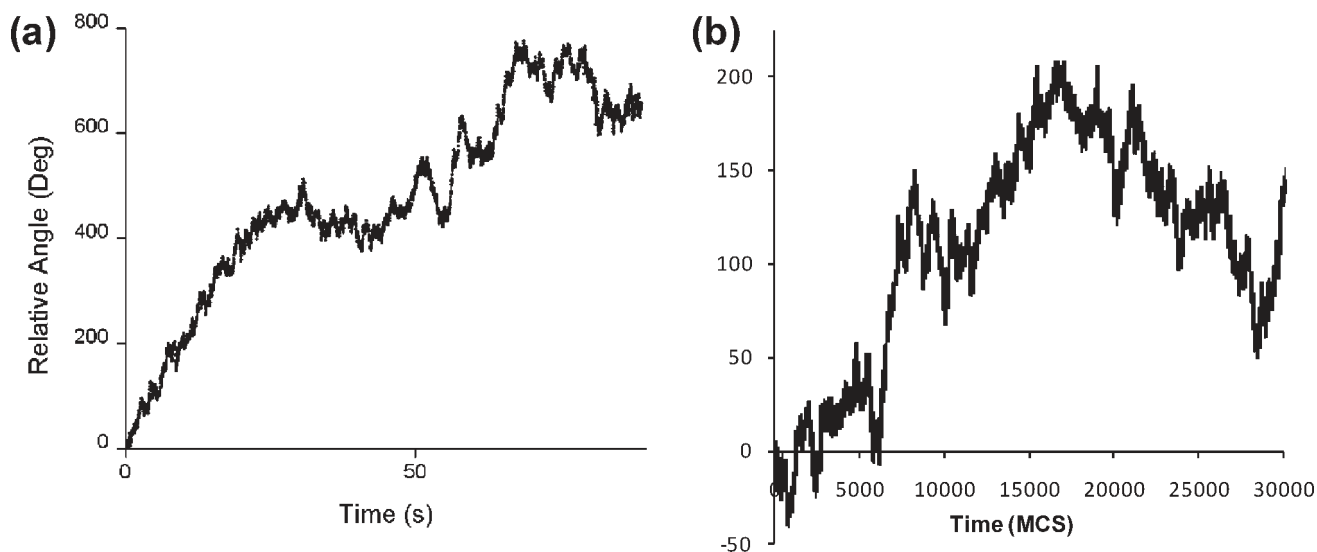


Figure 5. Relative angular position for (a) a single particle observed experimentally and for (b) a simulation of a random walk on a circle for 30000 Monte Carlo steps (MCS).

field, no observable change occurs as a result of one-dimensional rotational diffusion in the unrestricted dimension. Instead, orientation changes are observed when the particle fluctuates away from being aligned with the magnetic field. A sample measurement for 1.0 mT is shown in Figure 3a, where the deviation from alignment was found to be 3.9 degrees. This measurement was performed for various magnetic field strengths and the standard deviation from alignment with the applied magnetic field was found to decrease with increasing magnetic field — Figure 3b. The larger the magnitude of the magnetic field, the more the observed particle was confined. This general behavior is expected by the mB/kT energy consideration, where k is the Boltzmann constant, T the temperature, m the magnetic moment of the particle, and B the magnetic field amplitude. The $2\ \mu\text{m}$ particles with 100 nm Ni coating were estimated to have a magnetic moment of $4.4 \times 10^{-12}\ \text{Am}^2$, which in 1 mT magnetic

field at room temperature leads to $mB/kT \approx 10^6$. The overall behavior of the magnetic Janus particle magnetized through its poles is shown in Figure 3c (also see Video 1 in the Supporting Information).

As shown in Figure 1, standard bright-field microscopy was used to image the Janus particle. Figure 1b schematically illustrates how the optical asymmetry and magnetic anisotropy of a magnetic Janus particle is used to restrict the rotational diffusion to one axis, as well as to optically measure the rotation. The metallic capping has two important features: it introduces both optical and magnetic anisotropy to the otherwise symmetric and nonmagnetic particle. The ferromagnetic nickel allows the particle to be magnetized along the equator of the particle (this can be chosen during the fabrication steps; alternatively, the particles can also be magnetized along their poles). This magnetic orientation still allows for rotational diffusion, but only

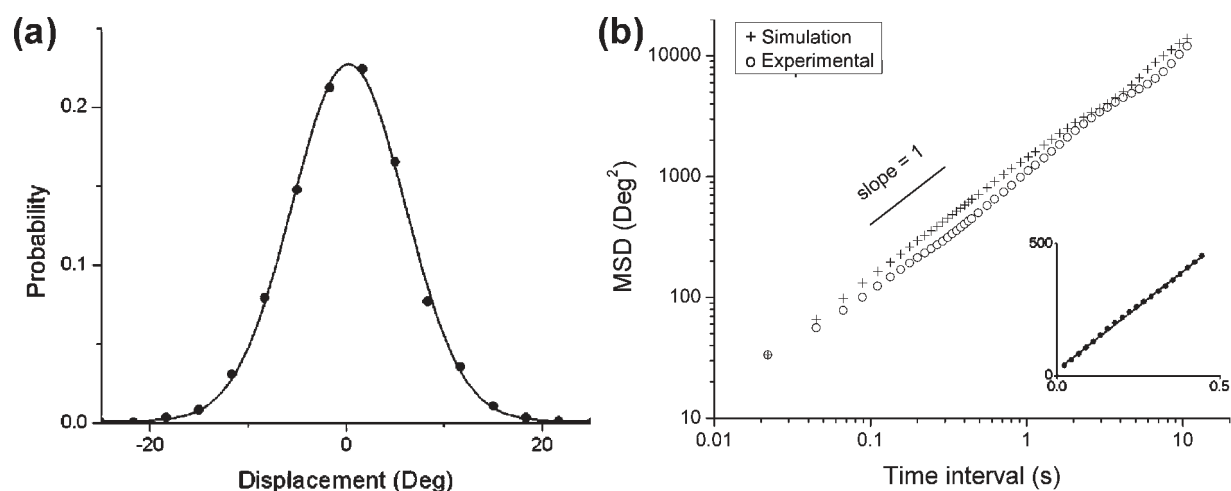


Figure 6. Experimental results for the particle relative angular position shown in Figure 5a for (a) the probability distribution function, where circles are data and the line is a Gaussian fit with a width of 5.70° ($D_r = 727.5 \text{ deg}^2/\text{s}$), and (b) the mean squared angular displacement (MSD), where the MSD plot shows every 10th data point and has a slope of $1195 \text{ deg}^2/\text{s}$. Inset: linear scale MSD plot for the first 20 data points, which has a slope of $965.0 \text{ deg}^2/\text{s}$.

about the one axis, when a field is applied. The reason for choosing the equator as the direction of magnetization is that the rotational diffusion can be observed via the optical asymmetry caused by the half-coating. With a set of Helmholtz coils the axis of rotational diffusion can be chosen to be parallel to the imaging plane or perpendicular to the imaging plane. Here we limited the rotational diffusion to being parallel to the imaging plane (magnetic field perpendicular to the imaging plane). This orientation was chosen to enable the direct measurement of the angle of orientation, as can be seen in the series of images in Figure 4 (also see Video 2 in the Supporting Information), and in order to limit any gravitational effects that can result from the center-of-mass of the particle being off center.

Figure 4 shows a time series of bright-field microscopy images resulting from one-dimensional rotational diffusion of a single typical magnetic Janus particle. The magnetic field is static along the optical axis (perpendicular to the imaging plane) and the magnetic Janus particle aligns itself in such a way that the equator of the particle is aligned with the field. This allows for unrestricted rotational diffusion only in the plane parallel to the imaging plane. By changing the direction of the static field, it is also possible to allow for rotational diffusion around different rotational axes, such as parallel to the imaging plane. Such a degree of control of rotational diffusion has not been demonstrated before. Being able to control how the particle rotationally diffuses with respect to an interface or object addresses the potential limitation of using the optical intensity to approximate the angle, as previously done for free rotational diffusion.^{22,29–31,39}

When the particle diffuses in the imaging plane as shown in Figure 4, it is straightforward to measure the time-dependent angular orientation of the particle. Figure 5a shows the relative angular orientation of a single typical particle over 90 s. From this data, the angular displacement can be calculated and the probability distribution can be determined — see Figure 6a. The fit is in good agreement with eq 3 and suggests normal Brownian diffusion for one-dimensional rotation. The mean squared angular displacement also corresponds to diffusion as described by eq 4. The diffusion coefficient, determined from the fit in Figure 6a, is $727.5 \text{ deg}^2/\text{s}$ (by using $\tau = 1/2D$, where τ is the rotational correlation time, we obtain $\tau = 2.26 \text{ s}$). This value is comparable to the reported value of 3.1 s for a $2 \mu\text{m}$ microsphere

in water.^{30,42} However, we do not expect exact agreement because of the unknown viscosity of the surfactant environment, and possibly due to the proximity of the Janus particle to the glass-fluid interface.^{43,44}

Finally, we demonstrate one potential useful application of actively restricting the Brownian rotation to a single dimension. We measured the rotational diffusion of a rigid four particle aggregate about two different axes: one with no applied field (“field off”) where the rotation was restricted by the glass-fluid interface, and the other with an applied magnetic field (“field on”), where the rotation was restricted by the field; see Figure 7a–f. The aggregate was formed by magnetic attraction after the particles were separately suspended in the fluid. The diffusion coefficients were calculated from the fits to be 21.7 and $90.2 \text{ deg}^2/\text{s}$ for the “field off” and “field on” conditions, respectively. These values are in the range of other rotational diffusion values for similarly sized aggregates.³¹ Since the aggregate is asymmetric, the diffusion coefficients are not equal around different axes, which we were able to measure by confining the rotation around one axis at a time. While the exact viscosity of the medium is unknown (due to the surfactant and proximity of the interface), this ratio does not depend on viscosity. The aggregate experiences a different amount of drag as it rotates about different axes. This can be easily seen by taking the ratio of the two diffusion coefficients

$$\frac{D_r^{\text{on}}}{D_r^{\text{off}}} = \frac{\gamma_{\text{off}}}{\gamma_{\text{on}}} \quad (5)$$

The change in drag can arise from either interface effects (e.g., effective viscosity) or from the difference in shape factor, κ . For the four particle aggregate shown in Figure 7, we observed a ratio of 4.15. This demonstrates that this method can indeed actively control and measure the rotational diffusion of a complex aggregate.

■ SIMULATIONS

In addition to the experiments and theoretical considerations discussed above we performed two types of computer simulations, which corroborated the experimental findings. In the first type, a rotational diffusion motion is modeled by a random walk,

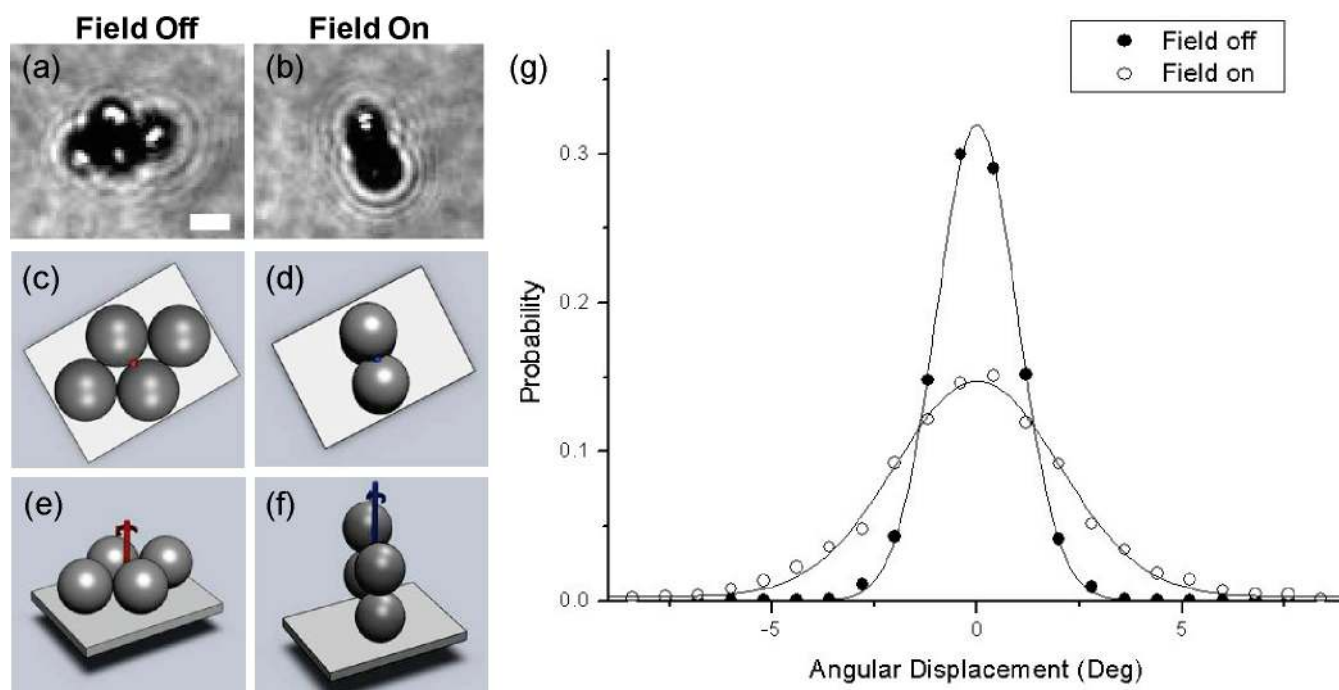


Figure 7. Optical microscopy images of a four particle aggregate with (a) no applied field and (b) a field applied along the optical axis (in the direction perpendicular to the imaging plane), where the scale bar is $2\ \mu\text{m}$. Schematic illustrations of the same aggregate oriented on the glass–fluid interface with the (c, e) “field off” (gravitational forces determine fixed axis) and (d, f) “field on” (magnetic forces determined fixed axis). (g) Angular displacement distribution function for the aggregate shown in (a) and (b), where the circles denote data and the line is a Gaussian fit. The width of the Gaussian fits were determined to be 0.98° and 2.0° , which give diffusion coefficients of 21.7 and $90.2\ \text{deg}^2/\text{s}$, respectively.

which is performed as a function of time, in the usual Monte Carlo method. The rotating system is simulated by a particle starting at some random initial position and performing a rotational motion, i.e. it rotates around one of its axes at angles whose directions are randomly chosen, in a way similar to when a particle performs a translational random walk on a lattice. One can then easily see that the one-dimensional rotational diffusion problem is equivalent to having a particle perform a random walk on the circumference of a circle, which in turn is equivalent to a random walk on a one-dimensional lattice, with a cyclic boundary condition, at the $2\pi r$ length of the circumference of the circle. When plotting the mean squared angular displacement vs time interval, we obtain Figure 6b, where the simulation data is normalized, so that the first data point agrees with the experimental data. Figure 6b shows a close agreement between experimental data and simulation. This illustrates that the experimental curves indeed represent unrestricted random rotations of the particles. Furthermore, the angular displacement distribution of the simulation also exhibits a Gaussian distribution, similar to the experimental findings (Figures 3b and 5a).

In the second type of simulations, the rotational diffusion tensor is calculated with the “Hydro++” software developed by Fernandes and de la Torre.^{45,46} The software can be used to calculate rotational properties and the intrinsic viscosity of any object that can be expressed with a list of Cartesian coordinates and radii of spheres. We implemented the hydrodynamic simulation (Hydro++) program to determine the diffusion tensor for a four particle aggregate in a diamond shape, similar to the aggregate shown in Figure 7g. The simulated ratio for a diamond shaped four particle aggregate gives a value for the ratio in eq 5 of 1.58. This is off by a factor of 2.62 from our measured value of

4.15, but this deviation may possibly be accounted for by interface effects, or viscosity effects, resulting from the surfactant mixture.

CONCLUSIONS

Summarizing, experimental systems that demonstrate one-dimensional Brownian rotation, i.e. Brownian rotation around a single conserved, fixed rotation axis, were designed and implemented. Reasonable values for the rotational diffusion coefficient were derived for the systems under investigation. In addition to single particles, we also monitored the one-dimensional rotational diffusion of a cluster of four particles. Our results show, even over long time periods (e.g., $\Delta t > \tau$), that the variation of the angle of rotation is indeed Brownian. The associated probability distribution function is Gaussian, and the mean squared angular displacement grows linearly with time. This is expected to be true only for one-dimensional rotation, but not for the noncommutative three-dimensional rotation. Further experimental work is needed for the three-dimensional case, but the differentiation between the one-dimensional and three-dimensional rotation is an important distinction that has been often overlooked in the past. The fact that we were able to make direct measurements on single particles provides a new method for handling rotational Brownian motion in a completely controlled way, which has not been reported thus far. Furthermore, Monte Carlo simulations agree well with the experimental results. One-dimensional rotational diffusion of a single particle was shown to behave as predicted by the Einstein 1906 model, and in complete analogy with translational Brownian motion. Thus, one-dimensional unrestricted rotational systems can be studied with this straightforward approach. This new methodology could also offer a new way for the study of rotational diffusion near interfaces. We also

demonstrated the potential application of isolating various axes of rotation in the case of a small particle aggregate.

■ ASSOCIATED CONTENT

S Supporting Information. Two additional videos showing a single magnetic Janus particles in a static magnetic field. This material is available free of charge via the Internet at <http://pubs.acs.org>.

■ ACKNOWLEDGMENT

The authors would like to acknowledge Rodney Agayan, Jeffrey Anker, and Dan Youngstrom for useful discussions. This work was supported by NSF/DMR Grant 0455330 (R.K.).

■ REFERENCES

- (1) Brown, R. *A brief account of microscopical observations: made in the months of June, July, and August, 1827, on the particles contained in the pollen of plants and on the general existence of active molecules in organic and inorganic bodies*; Printed by R. Taylor, 1828; Vol. 4.
- (2) Brown, R. *Additional remarks on active molecules*; Printed by R. Taylor, 1829; Vol. 6.
- (3) Einstein, A. *Ann. Phys.* **1905**, 322.
- (4) Einstein, A. *Ann. Phys.* **1906**, 19, 371–381.
- (5) Einstein, A. *Investigations on the Theory of the Brownian Movement*; Dover Publications: New York, 1956.
- (6) Perrin, J. *Brownian Movement and Molecular Reality*; Taylor and Francis: London, 1910.
- (7) Weiss, G. H.; Weiss, G. H. *Aspects and applications of the random walk*; North-Holland: Amsterdam, 1994.
- (8) Ben-Avraham, D.; Havlin, S. *Diffusion and reactions in fractals and disordered systems*; Cambridge University Press: New York, 2000.
- (9) Redner, S. *A guide to first-passage processes*; Cambridge University Press: New York, 2001.
- (10) Chandrasekhar, S. *Rev. Mod. Phys.* **1943**, 15, 1–89.
- (11) Browne, W. R.; Feringa, B. L. *Nat. Nanotechnol.* **2006**, 1, 25–35.
- (12) Berg, H. C. *Random walks in biology*; Princeton University Press: Princeton, NJ, 1993.
- (13) Furry, W. H. *Phys. Rev.* **1957**, 107, 7–13.
- (14) Altintas, E.; Boehringer, K.; Fujita, H. *IEIC Tech. Rep.* **2005**, 105, 51–54.
- (15) Altintas, E.; Bohringer, K. F.; Fujita, H. In *Solid-State Sensors, Actuators and Microsystems Conference, 2007. TRANSDUCERS 2007. International*; 2007; pp. 2239–2242.
- (16) Kappler, E. *Ann. Phys.* **1931**, 11, 233–256.
- (17) Cheng, Z.; Mason, T. G. *Phys. Rev. Lett.* **2003**, 90, 18304.
- (18) Cheng, Z.; Chaikin, P. M.; Mason, T. G. *Phys. Rev. Lett.* **2002**, 89, 108303.
- (19) Mukhija, D.; Solomon, M. J. *J. Colloid Interface Sci.* **2007**, 314, 98–106.
- (20) Anthony, S. M.; Kim, M.; Granick, S. *J. Chem. Phys.* **2008**, 129, 244701.
- (21) Takei, H.; Shimizu, N. *Langmuir* **1997**, 13, 1865–1868.
- (22) Anker, J. N.; Kopelman, R. *Appl. Phys. Lett.* **2003**, 82, 1102.
- (23) Perro, A.; Reculusa, S.; Ravaine, S.; Bourgeat-Lami, E.; Duguet, E. *J. Mater. Chem.* **2005**, 15, 3745–3760.
- (24) Anker, J. N.; Behrend, C.; Kopelman, R. *J. Appl. Phys.* **2003**, 93, 6698.
- (25) Anker, J. N.; Behrend, C. J.; McNaughton, B. H.; Roberts, T. G.; Brasuel, M.; Philibert, M. A.; Kopelman, R. *Mater. Res. Soc. Symp. Proc.* **1999**, 790, 17–28.
- (26) Behrend, C. J.; Anker, J. N.; McNaughton, B. H.; Kopelman, R. *J. Magn. Magn. Mater.* **2005**, 293, 663–670.
- (27) McNaughton, B. H.; Agayan, R. R.; Wang, J. X.; Kopelman, R. *Sens. Actuators: B. Chem.* **2007**, 121, 330–340.

- (28) McNaughton, B. H.; Agayan, R. R.; Clarke, R.; Smith, R. G.; Kopelman, R. *Appl. Phys. Lett.* **2007**, 91, 224105.
- (29) Behrend, C. J.; Anker, J. N.; Kopelman, R. *Appl. Phys. Lett.* **2004**, 84, 154.
- (30) Behrend, C. J.; Anker, J. N.; McNaughton, B. H.; Brasuel, M.; Philibert, M. A.; Kopelman, R. *J. Phys. Chem. B* **2004**, 108, 10408–10414.
- (31) Hong, L.; Anthony, S. M.; Granick, S. *Langmuir* **2006**, 22, 7128–7131.
- (32) Choi, J.; Zhao, Y.; Zhang, D.; Chien, S.; Lo, Y. H. *Nano Lett.* **2003**, 3, 995–1000.
- (33) McNaughton, B. H.; Stoica, V. A.; Anker, J. N.; Tyner, K. M.; Clarke, R.; Kopelman, R. *MRS Proc.* **2006**, 988, S99E.
- (34) Dhar, P.; Fischer, T. M.; Wang, Y.; Mallouk, T. E.; Paxton, W. F.; Sen, A. *Nano Lett* **2006**, 6, 66–72.
- (35) Rasband, W. S. *ImageJ*; U. S. Institutes of Health: Bethesda, MD, 1997–2005.
- (36) Favro, L. D. *Phys. Rev.* **1960**, 119, 53–62.
- (37) Hubbard, P. S. *Phys. Rev. A* **1972**, 6, 2421–2433.
- (38) Anthony, S.; Hong, L.; Kim, M.; Granick, S. *Langmuir* **2006**, 22, 9812–9815.
- (39) Brody, J. P.; Quake, S. R. *Appl. Phys. Lett.* **1999**, 74, 144.
- (40) Fernandes, M. X.; de la Torre, J. G. *Biophys. J.* **2002**, 83, 3039–3048.
- (41) Crocker, J. C. *J. Chem. Phys.* **1997**, 106, 2837.
- (42) Valberg, P. A.; Butler, J. P. *Biophys. J.* **1987**, 52, 537–550.
- (43) Lin, B.; Yu, J.; Rice, S. A. *Phys. Rev. E* **2000**, 62, 3909–3919.
- (44) Jones, R. B. *J. Chem. Phys.* **2005**, 123, 164705.
- (45) de la Torre, J. G.; Navarro, S.; Martinez, M. C. L.; Diaz, F. G.; Cascales, J. L. *Biophys. J.* **1994**, 67, 530–531.
- (46) de la Torre, J. G.; Echenique, G. D.; Ortega, A. *J. Phys. Chem. B* **2007**, 111, 955–961.
- (47) McNaughton, B. H.; Shlomij, I.; Kinnunen, P.; Cionca, C.; Pei, S. N.; Clarke, R.; Argyrakakis, P.; Kopelman, R. *Appl. Phys. Lett.* **2010**, 97, 144103.
- (48) Kinnunen, P.; Sinn, I.; McNaughton, B. H.; Kopelman, R. *Appl. Phys. Lett.* **2010**, 97, 223701.
- (49) Hecht, A.; Kinnunen, P.; McNaughton, B. H.; Kopelman, R. *J. Magn. Magn. Mater.* **2011**, 323, 272.
- (50) Sinn, I.; Kinnunen, P.; Pei, S. N.; Clarke, R.; McNaughton, B. H.; Kopelman, R. *Appl. Phys. Lett.* **2011**, 98, 024101.
- (51) Kinnunen, P.; Sinn, I.; McNaughton, B. H.; Newton, D. W.; Burns, M. A.; Kopelman, R. *Biosens. and Bioelectron* **2011**, 26, 2751.

■ NOTE ADDED IN PROOF

Five more relevant papers have been recently published (refs 47–51).